



Magnetically induced electric polarization in an organometallic magnet

V. S. Zapf,¹ M. Kenzelmann,² F. Wolff-Fabris,^{1,*} F. Balakirev,¹ and Y. Chen^{3,4,5}

¹National High Magnetic Field Laboratory (NHMFL), Los Alamos National Laboratory (LANL), Los Alamos, New Mexico 87545, USA

²Laboratory for Developments and Methods, Paul Scherrer Institute, CH-5232 Villigen, Switzerland

³Department of Physics and Astronomy, Johns Hopkins University, Baltimore, Maryland 21218, USA

⁴NIST Center for Neutron Research, National Institute of Standards and Technology, Gaithersburg, Maryland 20899, USA

⁵Department of Materials Science and Engineering, University of Maryland, College Park, Maryland 20742, USA

(Received 30 April 2009; revised manuscript received 23 June 2010; published 13 August 2010)

The coupling between magnetic order and ferroelectricity has been under intense investigation in a wide range of transition-metal oxides. The most direct coupling is obtained in so-called magnetically induced multiferroics where ferroelectricity arises directly from magnetic order that breaks spatial inversion symmetry. However, it has been difficult to find nonoxide-based materials in which these effects occur. Here we present a study of copper dimethyl sulfoxide dichloride (CDC), an organometallic quantum magnet containing $S = 1/2$ Cu spins, in which electric polarization arises from noncollinear magnetic order. We show that the electric polarization can be switched in a stunning hysteretic fashion. Because the magnetic order in CDC is mediated by large organic molecules, our study shows that magnetoelectric interactions can exist in this important class of materials, opening the road to designing magnetoelectrics and multiferroics using large molecules as building blocks. Further, we demonstrate that CDC undergoes a magnetoelectric quantum phase transition where both ferroelectric and magnetic order emerge simultaneously as a function of magnetic field at very low temperatures.

DOI: 10.1103/PhysRevB.82.060402

PACS number(s): 75.80.+q, 73.43.Nq, 77.22.Ej, 77.80.Fm

Magnetoelectric multiferroics are compounds with magnetic and electric orders that coexist and are coupled via magnetoelectric interactions.^{1–4} Research in this field is motivated by the promise of devices that can sense and create magnetic polarizations using electric fields and vice versa, thereby creating new functionality as well as improving the speed, energy efficiency, and size of existing circuits. A new class of induced multiferroics has become the topic of intense study in the past few years, in which a magnetic order induces an electric polarization.^{5–13} These materials are either low-dimensional or frustrated magnets in which competing interactions give rise to noncollinear order that breaks spatial inversion symmetry (SIS). This SIS-breaking magnetism couples to the lattice most likely via spin-orbit interactions that lower magnetic energy by distorting the lattice and in the process create electric polarization.

Most magnetoelectrics and multiferroics are transition-metal oxides or fluorides where the magnetoelectric interactions are mediated via superexchange through the oxide and fluoride anions. Magnetoelectric interactions can also be expected in other materials such as organometallic solids but have not yet been clearly established.^{14–16} In this paper we present field-induced multiferroic behavior in an organometallic quantum magnet, $\text{CuCl}_2 \cdot 2[(\text{CH}_3)_2\text{SO}]$ (CDC) where the Cu spins adopt noncollinear magnetic order that creates an electric polarization in the presence of magnetic fields. Unlike many magnetically induced multiferroics, the magnetic spins do not form a spiral in order to break SIS.

CDC crystallizes in an orthorhombic crystal structure with space-group $Pnma$ [see Fig. 1(a)].¹⁷ The Cu spins form zigzag chains in the crystallographic a - c plane, along which the Cu spins are antiferromagnetically coupled via a superexchange interaction $J=1.46$ meV mediated by Cl ions.¹⁸ Perpendicular to the chains, the Cu atoms are separated by

dimethyl sulfoxide groups [Fig. 1(b)] and it is this weaker antiferromagnetic (AFM) interaction that sets the energy scale for three-dimensional long-range order with a Néel temperature $T_N=0.9$ K.¹⁸ Figure 1(c) shows the evolution of the Cu spins with applied magnetic fields along the c axis, and the phase diagram is summarized in Fig. 2. At zero magnetic field H , the magnetic order consists of a collinear AFM arrangement (AFM A) with the magnetic moments pointing along the c axis. As a magnetic field is applied along the c axis, the spins undergo a first-order spin-flop transition into

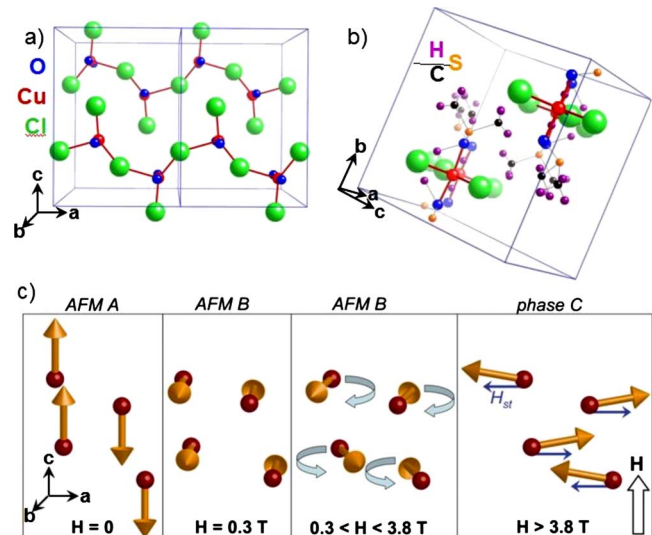


FIG. 1. (Color online) (a) Crystal structure of CDC showing the Cu-Cl chains. (b) Structure showing the organic molecules mediating exchange along the b axis. (c) Effect of applied magnetic fields on the spins (shown as arrows) of the Cu atoms (shown as balls) for one unit cell.

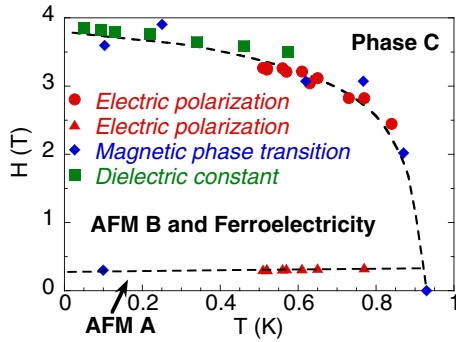


FIG. 2. (Color online) Magnetic field H -Temperature T phase diagram of CDC showing regions of collinear and noncollinear antiferromagnetism (AFM A and B), ferroelectricity, and the staggered paramagnetism (phase C) that occurs at high fields for H along [001]. Data are obtained from peaks in the dielectric constant and magnetoelectric current (this work), neutron diffraction, (Ref. 18) and specific heat (Ref. 19).

the b axis at 0.3 T. As H is increased further, effective local magnetic fields appear on the Cu sites that alternate from one site to the next along the a axis, and whose strength is proportional to the external magnetic field. These effective fields result from spin-orbit couplings, namely, a staggered g tensor and a Dzyaloshinskii-Moriya interaction.¹⁹ The effective magnetic fields are shown as small blue arrows in the final panel of Fig. 1(c). In response to these staggered fields, the spins gradually rotate from the b axis to the a axis and become noncollinear in the process (AFM B). Between $H = 0.3$ and 3.8 T, the magnetic structure is thus described by two order parameters, one due to the AFM superexchange interactions between the Cu spins and the other due to the spin-orbit-induced staggered fields. Finally, the spins align with the staggered fields along the a axis for $H_c > 3.8$ T (phase C). In addition to the behavior described so far, the spins also cant along the magnetic field direction with increasing field.

We can show that the noncollinear state between 0.3 and 3.8 T (AFM B) breaks SIS and thereby allows an electric polarization P to occur along the b axis. At zero field (AFM A) the magnetic order is commensurate with a wave vector $k=(0,0,0)$. Thus the space group of the magnetic ordering matches that of the lattice, which has eight irreducible representations $\Gamma^1-\Gamma^8$.¹⁹ In order to compute whether an electric polarization is possible, we can write down a Landau Hamiltonian with trilinear coupling $\mathcal{H}=P\cdot L_1\cdot L_2$, where L_1 is the magnetization along the b axis that is stabilized by long-range order and $L_2=\chi H$ results from the effective staggered local magnetic fields along the a axis.

The Hamiltonian \mathcal{H} must be invariant under all symmetry operations of the space group, and thus P must transform as $L_1\cdot L_2$. L_1 belongs to Γ^5 and L_2 belongs to Γ^8 , thus P transforms as $\Gamma^5\times\Gamma^8$. As can be seen in Table I, $\Gamma^5\times\Gamma^8$ contains a single broken mirror plane (m_{ac}) implying an allowed uniform P along the b axis. Note that P is a uniform vector field with $Q=0$, and thus invariant under translation, so the glide operation m_{ac} reduces to a simple mirror reflection in the b axis. In this work we present measurements of the electric

TABLE I. Partial list of the irreducible representations of the group G_k for CDC with a commensurate magnetic structure with $k=(0,0,0)$. $\bar{1}$ is an inversion about the origin, 2_α denotes a screw axis along $\alpha=a,b,c$ (180° rotation followed by a translation), and $m_{\alpha,\beta}$ is a glide plane containing the axis α and β (mirror reflection in the plane α,β followed by a translation in that plane).

| | 1 | 2_b | 2_a | 2_c | $\bar{1}$ | m_{ac} | m_{bc} | m_{ab} |
|--------------------------|---|-------|-------|-------|-----------|----------|----------|----------|
| Γ^5 | 1 | -1 | 1 | -1 | -1 | 1 | -1 | 1 |
| Γ^8 | 1 | -1 | -1 | 1 | 1 | -1 | -1 | 1 |
| $\Gamma^5\times\Gamma^8$ | 1 | 1 | -1 | -1 | -1 | -1 | 1 | 1 |

properties of CDC and we show that an electric polarization indeed occurs along the b axis and is closely coupled to the noncollinear AFM B state.

Single-crystal samples of CDC were grown from solution.¹⁹ For $P(H)$ measurements, the samples were coated on the a - c faces with silver paint and leads were attached, permitting the magnetoelectric current along the b axis to be recorded with a Stanford Research 570 current to voltage converter. Measurements were performed during the up-sweep of magnetic field pulses with applied magnetic fields along the c axis. The samples were cooled by immersion in ^3He while rapid 10 T magnetic pulses with dB/dt up to 3.8 kT/s were applied using a short-pulse capacitively driven magnet at the National High Magnetic Field Laboratory in Los Alamos, NM (a large dB/dt increases the signal to noise levels). The dielectric constant was measured capacitatively in the liquid mixing chamber of an Oxford Kelvinox 400 ^3He - ^4He dilution refrigerator. In order to rule out possible magnetostriction affecting the dielectric constant measurements, magnetostriction was measured separately using a titanium dilatometer mounted in vacuum to the cold finger of the same dilution refrigerator.^{20,21} No signatures of the 3.8 T transition were observed with a sensitivity to magnetostriction effects $10\times$ greater than that of the dielectric constant measurements.

$P(H)$ of CDC along the b axis and the magnetoelectric current I from which it was derived are shown in Figs. 3(a) and 3(b). The data are shown for a series of magnetic field pulses along the positive and negative c axis (A through G) applied at $T=0.5$ K while P is measured along the b axis. $P(H)$ has a dome shape for applied magnetic fields between 0.3 and 3.8 T, indicating that P coexists with the noncollinear AFM B phase. In the magnetoelectric current data of Fig. 3(b), the feature at 0.3 T is sharp and first-order like whereas the transition near 3.8 T appears to be second order.

We expect P to result from SIS, so it is useful to compare $P(H)$ to the field dependence of this symmetry breaking. In Fig. 4 we extract the two magnetic order parameters L_1 (staggered M along b axis from AFM couplings) and L_2 (staggered M along the a axis resulting from spin-orbit interactions) from elastic neutron data. This is an expanded view of results presented in Ref. 19. The magnetic field evolution of magnetic Bragg peaks for various Q vectors are shown in Fig. 4(a). We fit the intensity vs magnetic field to the scenario summarized in Fig. 1. From this we can estimate the two individual magnetic order parameters L_1 and L_2 . These

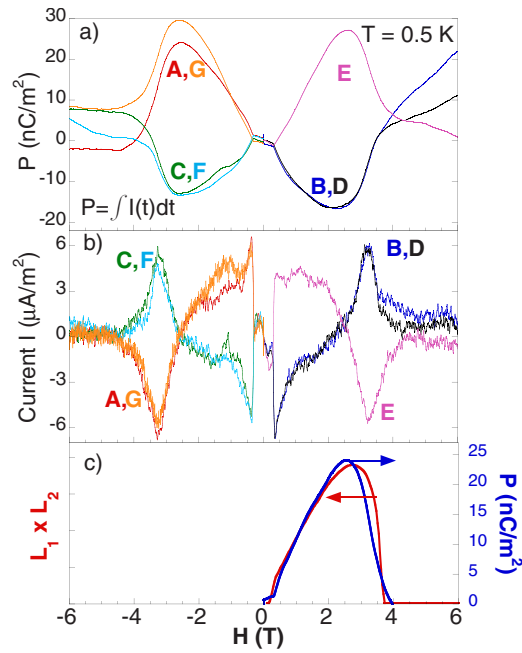


FIG. 3. (Color online) (a) Electric polarization P along the b axis vs magnetic field H along the c axis collected during a sequence of seven magnetic field pulses (A–G) at 0.5 K. (Data are shown only for rising fields.) (b) Magneto-electric current I vs H . (c) Comparison of $P(H)$ and the degree of SIS breaking (see text).

are shown in Fig. 4(b) as a function of magnetic field. The product of these two is a measure of the degree of SIS or can alternatively be thought of as the degree of noncollinearity of the spins. Thus in Fig. 3(c), we compare $P(H)$ to $L_1 \cdot L_2$. The correspondence between these two provides evidence that P is generated by the SIS breaking noncollinear magnetic order.

The direction of P can switch depending on the history of the magnetic field pulses, which demonstrates that it is ferroelectric. When two consecutive magnetic field pulses are applied along the same direction in the c axis [e.g., D followed by E or F followed by G in Fig. 3(a)], the resulting electric polarization for E and G is “positive” along the b axis. (The definition of positive and negative is arbitrary). On the other hand, when two consecutive pulses are applied in opposite directions along the c axis (A and B, B and C, C and D, and E and F), the resulting electric polarization for B, C, D, and F is switched into the “negative” direction along the b axis. These measurements were repeated for three samples and found to be reproducible. This type of switching behavior, where the direction of P depends both on the direction of the present magnetic field pulse and the previous one, is unique as far as we know among magnetoelectrics. We note that in addition to the sample being intrinsically hysteretic, there must also be a symmetry-breaking electric field along the b axis in order for the behavior described above to occur. This is further supported by the fact that no electric field poling is required to observe P . We speculate that this could result from the influence of Schottky voltages where the capacitor plates contact the sample. These do not contribute a background signal to the data since they are magnetic field independent, however, they can subject the crystal to a

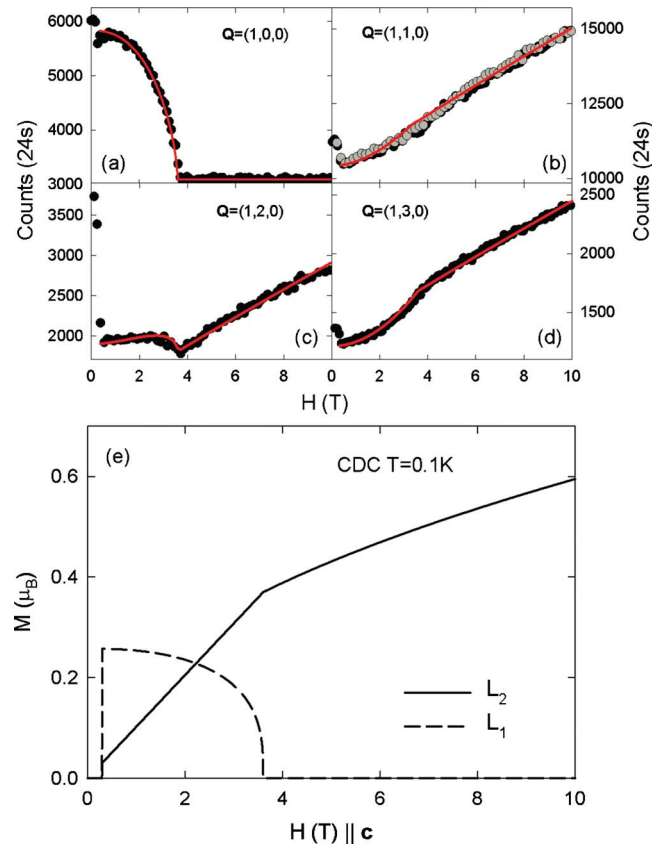


FIG. 4. (Color online) (a) Field dependence of magnetic peak intensities for four different Q vectors at 0.1 K. Red lines are fits to the magnetic spin configurations depicted in Fig. 1(c) and described in Ref. 19. (b) Based on the data in panel (a), we extract the field dependence of L_1 and L_2 .

symmetry-breaking electric field along b . The absence of external electric field poling required to observe P has previously been reported in the magnetoelectric compounds LiNiPO_4 and LiCoPO_4 .²²

The existence of an electric phase transition is confirmed by dielectric constant measurements along the b axis [Fig. 5(a)]. The signature of the phase transition is a peak in the dielectric constant near $H = 3.8$ T. The evolution of the peaks in the dielectric constant [Fig. 5(a)] and the magneto-electric current [Fig. 5(b)] with temperature are plotted in the phase diagram in Fig. 2 along with previous neutron scattering and specific-heat results.^{18,19} The excellent agreement between the region of noncollinear magnetic order (AFM B) and P in Fig. 2 is evidence for the coexistence and intimate coupling between the electric and magnetic properties of CDC.

Our measurements show that at the upper boundary of the H - T phase diagram in Fig. 2, magnetic order and electric polarization are suppressed simultaneously in a continuous phase transition as a function of magnetic field. This transition is not driven by temperature fluctuations, as it occurs at very low temperatures where temperature fluctuations are basically absent. Instead, an earlier work showed that the transition is the result of magnetic field-tuned quantum fluctuations that are associated with a quantum critical point at

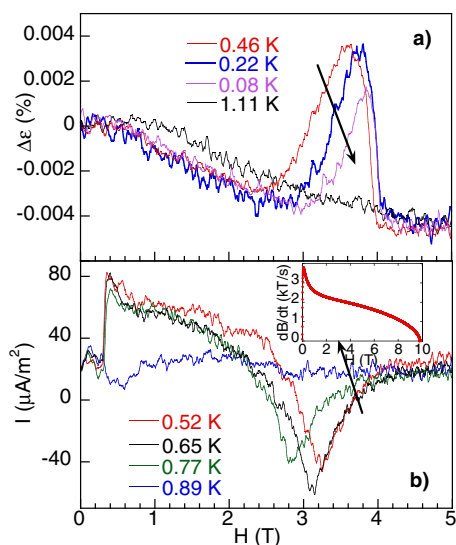


FIG. 5. (Color online) (a) Percentage change in the dielectric constant ϵ and rate of change in magnetic field dB/dt . (b) Magneto-electric current measurements vs applied magnetic field showing the transitions into and out of the ferroelectric phase. Inset: rate of change in magnetic field as a function of field during a 10 T pulse.

$H=3.8$ T.¹⁹ Specific-heat measurements yielded critical exponents approaching those of a three-dimensional Ising magnet with effective dimensionality $D=d+z=4$, where $d=3$ is the spatial dimension and $z=1$ is the dynamical exponent. This is contrast to an ordinary thermal Ising phase transition with $D=d=3$.

Our present study shows that an electric polarization emerges at the magnetic quantum critical point. The presence of a peak in the dielectric constant confirms that P undergoes an actual phase transition whose order parameter is coupled to the magnetic ones. Thus we can identify the phase transition as a function of magnetic field as a magneto-electric quantum critical point. Quantum critical points have been

investigated for cases where one order parameter is critical at the critical point, but we are not aware of any previously observed multiorder quantum critical point in solid matter. Our observation of a magneto-electric quantum critical point holds the promise of the study of novel physics in solid materials, such as exotic quantum phases in which two or more order parameters are intimately coupled. Taking advantage of the cross-coupling of two order parameters at a simultaneous critical point, it can be imagined that a magnetic critical point can be tuned with electric fields and vice versa. This adds new ways of conducting time-resolved studies of quantum critical phenomena using the next generation light sources, because electric fields can be controlled on a much smaller time scale than magnetic fields.

In summary, we demonstrate that magneto-electric interactions mediated via large molecules produce magnetically induced ferroelectricity. The ferroelectric polarization can be switched by short magnetic field pulses in an unusual hysteretic fashion. This initial study, while at low temperatures and with relatively small P , provides a motivation for future molecule-based designer magnets based on a wider range of organic ligands with which desired magneto-electric properties can be fine tuned. The organic ligands provide an array of structures that can lead to frustration and inversion-symmetry breaking including triangles and spirals,^{23–25} as well as polar bonds that can form significant electric polarizations,²⁶ coupled to the magnetic subsystem via the soft crystal structure. Finally, the observation of a magneto-electric quantum phase transition illustrates the scope of novel physics to be studied in organic magnets.

Work at the National High Magnetic Field Laboratory was supported by the U.S. National Science Foundation through Cooperative Grant No. DMR901624, the State of Florida, and the U.S. Department of Energy. Work at Johns Hopkins University was supported by the National Science Foundation through Grant No. DMR-0306940.

*Present address: Dresden Hoch-feld Labor, Dresden D-01328, Germany.

¹M. Fiebig, *J. Phys. D* **38**, R123 (2005).

²D. I. Khomskii, *J. Magn. Magn. Mater.* **306**, 1 (2006).

³W. Eerenstein *et al.*, *Nature (London)* **442**, 759 (2006).

⁴N. Hill, *J. Phys. Chem. B* **104**, 6694 (2000).

⁵T. Kimura *et al.*, *Nature (London)* **426**, 55 (2003).

⁶T. Goto, T. Kimura, G. Lawes, A. P. Ramirez, and Y. Tokura, *Phys. Rev. Lett.* **92**, 257201 (2004).

⁷N. Hur *et al.*, *Nature (London)* **429**, 392 (2004).

⁸G. Lawes *et al.*, *Phys. Rev. Lett.* **95**, 087205 (2005).

⁹H. Katsura, N. Nagaosa, and A. V. Balatsky, *Phys. Rev. Lett.* **95**, 057205 (2005).

¹⁰S. Cheong and M. Mostovoy, *Nature Mater.* **6**, 13 (2007).

¹¹M. Kenzelmann *et al.*, *Phys. Rev. Lett.* **98**, 267205 (2007).

¹²T. Arima, *J. Phys. Soc. Jpn.* **76**, 073702 (2007).

¹³T. Kimura, *Annu. Rev. Mater. Res.* **37**, 387 (2007).

¹⁴H.-B. Cui *et al.*, *J. Am. Chem. Soc.* **128**, 15074 (2006).

¹⁵Q. Ye *et al.*, *Inorg. Chem.* **47**, 772 (2008).

¹⁶J. F. Scott, *J. Phys.: Condens. Matter* **20**, 021001 (2008).

¹⁷R. D. Willett and K. Chang, *Inorg. Chim. Acta* **4**, 447 (1970).

¹⁸M. Kenzelmann, Y. Chen, C. Broholm, D. H. Reich, and Y. Qiu, *Phys. Rev. Lett.* **93**, 017204 (2004).

¹⁹Y. Chen, M. B. Stone, M. Kenzelmann, C. D. Batista, D. H. Reich, and C. Broholm, *Phys. Rev. B* **75**, 214409 (2007).

²⁰V. S. Zapf *et al.*, *Phys. Rev. B* **77**, 020404(R) (2008).

²¹G. M. Schmiedeshoff *et al.*, *Rev. Sci. Instrum.* **77**, 123907 (2006).

²²I. Kornev, M. Bichurin, J.-P. Rivera, S. Gentil, H. Schmid, A. G. M. Jansen, and P. Wyder, *Phys. Rev. B* **62**, 12247 (2000).

²³S. J. Lee *et al.*, *J. Am. Chem. Soc.* **124**, 12948 (2002).

²⁴F. A. Cotton *et al.*, *Inorg. Chem.* **43**, 8394 (2004).

²⁵M. J. Hannon *et al.*, *Chem.-Eur. J.* **8**, 2225 (2002).

²⁶G. J. Goldsmith and J. G. White, *J. Chem. Phys.* **31**, 1175 (1959).